Vibrational branching ratios and shape resonant photoionization dynamics in N_2O

M. Braunstein and V. McKoy
Arthur Amos Noyes Laboratory of Chemical Physics,[a] *California Institute of Technology, Pasadena, California 91125*

(Received 15 September 1988; accepted 28 October 1988)

Vibrational branching ratios and photoelectron asymmetry parameters for alternative vibrational modes in the photoionization of $N_2O(7\sigma^{-1})$ have been studied using accurate photoelectron continuum orbitals. Earlier dispersed ionic fluorescence measurements [E. D. Poliakoff, M. H. Ho, M. G. White, and G. E. Leroi, Chem. Phys. Lett. **130**, 91 (1986)] revealed strong non-Franck–Condon vibrational ion distributions for both the symmetric and antisymmetric stretching modes at low photoelectron energies. Our results establish that these features arise from a σ shape resonance which, based on its dependence on internuclear geometry, must be associated with the molecular framework as a whole and not with either of its fragments, N–N or N–O. This behavior accounts for the more pronounced deviations of the vibrational branching ratios from Franck–Condon values observed in the symmetric than in the antisymmetric mode. The σ continuum also supports a second shape resonance at higher energy which does not influence the vibrational branching ratios but is quite evident in the photoelectron asymmetry parameters around a photon energy of 40 eV. These vibrationally resolved studies of the photoelectron spectra of this polyatomic system provide an interesting example of the rich shape resonant behavior that can be expected to arise in polyatomic molecules with their alternative vibrational modes.

I. INTRODUCTION

Shape resonant features have been studied in the photoionization spectra of a wide range of molecules.[1] One of the more significant dynamical features arising in molecular photoionization cross sections from such resonances is the non-Franck–Condon behavior seen in the vibrationally resolved photoelectron spectra where the ionic vibrational distribution is no longer given simply by Franck–Condon factors and photoelectron angular distributions depend on the vibrational level. This breakdown of the Franck–Condon principle, first identified by Dehmer *et al.*[2] in the N_2 spectra and subsequently studied both experimentally and theoretically by others,[3–5] is due to the strong dependence of the position and lifetime of the resonance on internuclear separation and is obviously an important probe of photoelectron dynamics. Much of our physical understanding of the role of shape resonances in vibrationally resolved photoelectron spectra is based on the simple picture of their behavior in diatomics,[2] i.e., shifts to higher energies with shorter bond distances. With their alternative vibrational modes and the possibility of shape resonances associated with specific bonds in the molecule, as well as intramolecular interaction among such resonances,[6] shape resonant behavior in polyatomics can be expected to be potentially richer than in the simpler diatomic molecules. Vibrationally resolved studies are required to probe the behavior of shape resonances with alternative internuclear configurations.

Recently, Poliakoff *et al.*,[7] using dispersed ionic fluorescence—a technique which shows considerable promise for studies of vibrationally resolved photoelectron spectra of polyatomic molecules—have measured branching ratios for the (1,0,0) and (0,0,1) vibrational levels, the symmetric and antisymmetric stretching modes,respectively, of the $A\,^2\Sigma^+(7\sigma^{-1})$ state of N_2O^+ for photoelectron energies ranging from about 0.5 to 5 eV. These branching ratios were seen to be dependent on excitation energy, implying a breakdown of the Franck–Condon approximation. More recent ion fluorescence studies and photoelectron measurements of Kelly *et al.*[8] and Ferrett *et al.*,[9] respectively, at higher energy also show significant non-Franck–Condon branching ratios for these vibrational levels, particularly in the symmetric stretching mode. Earlier vibrationally unresolved studies[10] of the 7σ photoionization of N_2O identified two shape resonances in the σ ionization continuum, a low-energy pronounced resonance centered around 20 eV—the 7σ ionization potential is about 16.4 eV—responsible for the non-Franck–Condon vibrational branching ratios seen by Poliakoff *et al.*,[7] and a higher energy one around 38 eV which is essentially not evident in either the vibrationally resolved or unresolved cross sections but leads to a broad minimum in the photoelectron asymmetry parameters.

In this paper we present the results of vibrationally resolved studies of the cross sections and photoelectron asymmetry parameters for photoionization of the 7σ level in N_2O in the region of these two shape resonances. An important objective of these studies is to obtain some insight into the behavior of shape resonances for alternative internuclear configurations in a polyatomic molecule and hence their influence on specific vibrational branching ratios. For example, in a molecule such as N_2O do the shape resonances seen around 20 and 38 eV "belong" primarily to specific regions

[a] Contribution No. 7858.

 0021-9606/89/031535-09$02.10

of the molecule, i.e., N–N or N–O bonds, or would their behavior at different internuclear configurations suggest that they belong to the molecule as a whole? The answer to this question would obviously determine the influences these resonances can be expected to have on the branching ratios for symmetric and antisymmetric stretching modes. What we do find, perhaps in contrast to the more intuitive notion that these resonances in N_2O, particularly the low-energy one, should be associated with the localized N–N or N–O region of the molecule, is that they behave as though they belong to the molecule as a whole. As a result we expect that the shape resonance at 20 eV would more strongly influence the vibrational branching ratios for the symmetric stretch than for the antisymmetric stretch. In fact, although our calculated vibrational branching ratios show non-Franck–Condon behavior for both vibrational modes, the deviations are much more pronounced in the symmetric mode, in agreement with what is seen experimentally.[7–9]

An outline of the remaining sections of this paper is as follows. In Sec. II we briefly discuss the method we use to obtain the molecular photoelectron orbitals needed to determine the photoionization cross sections. In this section we also discuss the vibrational wave functions used. In Sec. III we present the results of fixed-nuclei calculations at 16 internuclear geometries. In Sec. IV our vibrationally resolved cross sections are discussed and compared with available experimental data.

II. METHOD AND CALCULATIONS

In these studies of the photoionization cross sections we use a Hartree–Fock wave function for the initial state. For the final state we use a frozen-core model in which the bound orbitals are assumed identical to those in the initial state Hartree–Fock wave function and the photoelectron wave function is determined in the field of these $(N-1)$ unrelaxed core orbitals. The static-exchange photoelectron continuum orbital then satisfies the one-electron Schrödinger equation,

$$(-1/2\nabla^2 + V_{N-1}(\mathbf{r},R) - k^2/2)\phi_{\mathbf{k}}(\mathbf{r},R) = 0, \quad (1)$$

where $V_{N-1}(\mathbf{r},R)$ is the nonlocal, nonspherical ion core potential, $k^2/2$ is the photoelectron kinetic energy, R denotes the internuclear geometry and $\phi_{\mathbf{k}}$ satisfies the appropriate boundary conditions. If $\phi_{\mathbf{k}}$ is expanded in spherical harmonics defined about $\hat{k}$, i.e.,

$$\phi_{\mathbf{k}}(\mathbf{r},R) = \left(\frac{2}{\pi}\right)^{1/2} \sum_{lm} i^l \varphi_{klm}(\mathbf{r},R) Y^*_{lm}(\hat{k}), \quad (2)$$

the functions $\varphi_{klm}(\mathbf{r},R)$ satisfy the same Schrödinger equation as $\phi_{\mathbf{k}}$ itself. We will discuss our procedure for solving Eq. (1) for these functions φ_{klm} later. With these functions φ_{klm} we define the length and velocity forms of the photoelectron matrix element as

$$I^L_{lm\mu}(R) = k^{1/2}\langle \phi_{7\sigma}(\mathbf{r},R)|r_\mu|\varphi_{klm}(\mathbf{r},R)\rangle, \quad (3)$$

$$I^V_{lm\mu}(R) = (k^{1/2}/E)\langle \phi_{7\sigma}(\mathbf{r},R)|\nabla_\mu|\varphi_{klm}(\mathbf{r},R)\rangle, \quad (4)$$

where $\phi_{7\sigma}$ is the occupied 7σ level of N_2O and E is the photon energy. The vibrationally resolved photoionization cross section $\sigma(v,v')$ can then be written as

$$\sigma^{L,V}_{v=0,v'=n} = \frac{4\pi^2}{3c} E \sum_{lm\mu} |\langle \chi_i^{v=0}(R)|I^{L,V}_{lm\mu}(R)|\chi_f^{v'=n}(R)\rangle|^2, \quad (5)$$

where χ_i and χ_f are vibrational wave functions for N_2O and N_2O^+, respectively, and c is the speed of light. The corresponding photoelectron asymmetry parameter is defined as

$$\frac{d\sigma^{L,V}_{v=0,v'=n}}{d\Omega_{\hat{k}}} = \frac{\sigma_{v=0,v'=n}}{4\pi}\left[1 + \beta^{L,V}_{v=0,v'=n} P_2(\cos\theta)\right], \quad (6)$$

where θ is the angle between the polarization vector of the light and the photoelectron momentum $\hat{k}$.

To obtain the photoelectron continuum orbital $\varphi_{klm}(\mathbf{r},R)$, φ_{klm} is further expanded in spherical harmonics, $Y_{l'm}(\hat{r})$. The resulting coupled equations are solved using an adaption of the Schwinger variational principle for long-range potentials in which the direct component V_{dir} of the molecular ion potential V_{N-1} is treated exactly by numerical integration and the exchange interaction V_{ex} is approximated by a separable form of the potential of the Schwinger type, i.e.,

$$V_{\text{ex}} \cong V^s_{\text{ex}} = \sum_{ij} V_{\text{ex}}|\alpha_i\rangle (V^{-1}_{\text{ex}})_{ij} \langle\alpha_j| V_{\text{ex}}, \quad (7)$$

where α_i are discrete basis functions. The approach yields variationally stable photoionization cross sections and includes an iterative procedure for obtaining the converged scattering solutions, φ_{klm}.[11] We have shown that the method can provide good approximations to the photoelectron orbitals even with modest expansions in Eq. (7).[11] For the expansion in Eq. (7) in these studies we used the basis shown in Table I of Ref. 10. With this basis the "zero-order" solutions were essentially converged and it was not necessary to resort to an iterative procedure. All matrix elements arising in the equations associated with this procedure are evaluated via single-center expansions about the central nitrogen atom and a Simpson's rule quadrature. The partial wave expansion parameters and the grids for the Simpson's rule quadrature of the radial integrals used here are the same as those given in Ref. 10.

For the ground state of N_2O, with an electron configuration $1\sigma^2 2\sigma^2 3\sigma^2 4\sigma^2 5\sigma^2 6\sigma^2 1\pi^4 7\sigma^2 2\pi^4$, we used the Slater basis SCF wave functions of McLean and Yoshimine[12,13] for the 16 internuclear distances at which we obtained the photoionization cross sections. At four of these geometries the wave functions were taken from Ref. 12. The wave functions at the other geometries were kindly provided by McLean.[13] At the N–N and N–O equilibrium bond distances of 2.1273 and 2.2418 a.u., respectively, this basis gives an SCF energy of $-183.756\,68$ a.u.

TABLE I. Force constants for N_2O and $N_2O^+(7\sigma^{-1})$ used in Eq. (8).[a]

	N_2O	$N_2O^+(7\sigma^{-1})$
k_{11}	18.01[b]	19.33
k_{22}	11.33	13.93
k_{12}	0.71	0.07

[a] Reference 14.
[b] In units of 10^5 dyn cm^{-1}

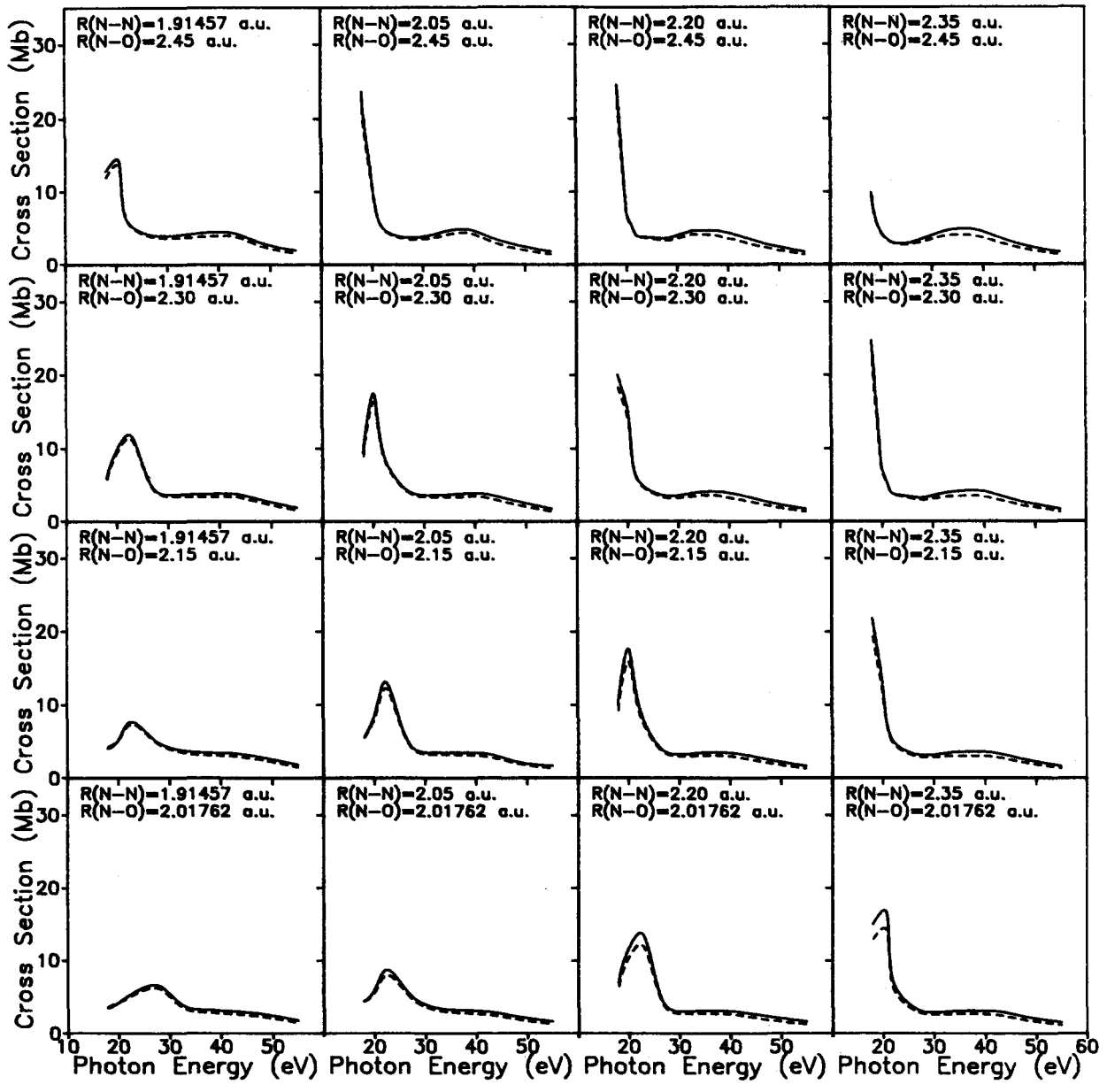

FIG. 1. Calculated cross sections (Mbs) for photoionization of the 7σ level of N_2O: —, total cross section (dipole length); ---, total cross section (dipole velocity). Along the horizontal axis from left to right, each frame corresponds to an N–N internuclear distance of 1.914 57, 2.05, 2.2, and 2.35 a.u., respectively. Along the vertical axis from bottom to top, each frame corresponds to an N–O internuclear distance of 2.017 62, 2.15, 2.3, and 2.45 a.u., respectively. The photon energy scale here and in Figs. 2 and 3 assumes an ionization potential of 16.4 eV (1 Mb $= 10^{-18}$ cm^2).

The vibrational wave functions for the symmetric and antisymmetric stretching modes of the ground state of N_2O and the $A\,^2\Sigma^+$ state of N_2O^+ were obtained by solving the vibrational Schrödinger equation for a nonbending, nonrotating linear triatomic molecule. Highly accurate potentials have not been determined for the $A\,^2\Sigma^+$ state for N_2O^+. For this state and for the ground state we hence used effective harmonic force fields with potentials of the form

$$2V = k_{11}\Delta r(\text{N–N})^2 + k_{22}\Delta r(\text{N–O})^2 + 2k_{12}\Delta r(\text{N–N})\Delta r(\text{N–O}), \quad (8)$$

where $\Delta r(\text{N–N}) = R(\text{N–N}) - R_e(\text{N–N})$, $\Delta r(\text{N–O}) = R(\text{N–O}) - R_e(\text{N–O})$. The values of the force constants, taken from Callomon and Creutzberg,[14] are listed in Table I. The form of the kinetic energy operator is given by Wilson *et al.*[15] The vibrational wave functions were expanded in a basis of the form $\Phi_{ij} = \phi_i(R_{\text{N-N}})\phi_j(R_{\text{N-O}})$ with the bond displacement functions ϕ_i chosen as harmonic oscillator functions. Diagonalization of the vibrational Hamiltonian in such a product basis containing the first five harmonic oscillator functions gave converged solutions. The resulting Franck–Condon factors were (000,000) = 0.583, (000,100) = 0.198, and (000,001) = 0.099. These vibrational wave functions for this polyatomic molecule obtained using harmonic potentials can certainly be expected to be of lower quality than for other ions for which more refined potentials are available. Measurements of the vibrational branching ratios at high photoelectron energies would be

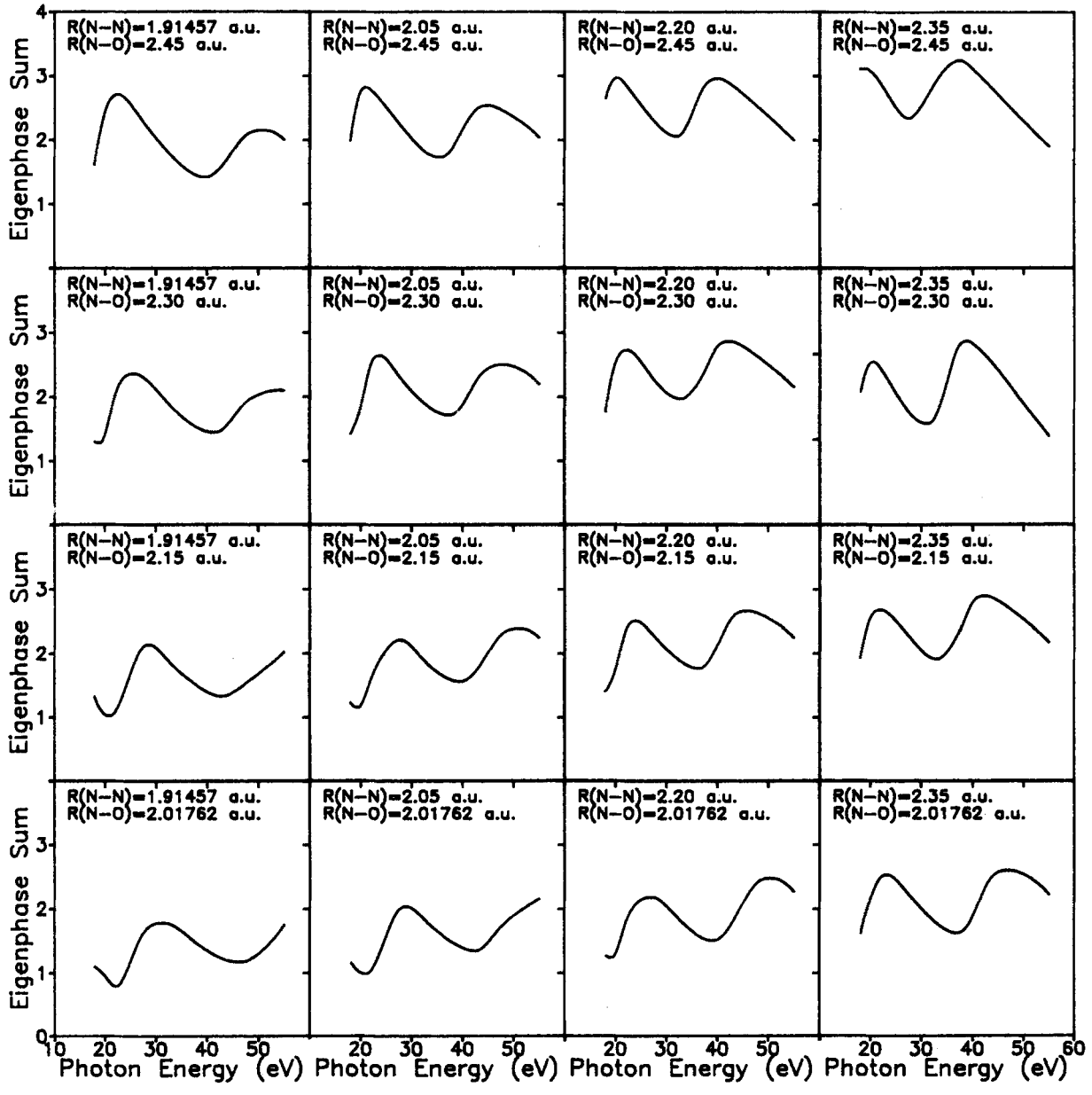

FIG. 2. Eigenphase sums in radians at several internuclear configurations for the $7\sigma \rightarrow k\sigma$ channel in N_2O. Each frame corresponds to the geometry described in Fig. 1.

useful in assessing the accuracy of the calculated Franck–Condon factors.

The photoelectron matrix elements $I_{lm\mu}(R)$ of Eqs. (3) and (4) were determined at 16 internuclear geometries chosen as points of a 4×4 grid with $R_{N\text{-}N} = 1.914\,57$, 2.05, 2.2, and 2.35 a.u. and $R_{N\text{-}O} = 2.017\,62$, 2.15, 2.3, and 2.45 a.u. The real and imaginary parts of the photoelectron matrix elements at these internuclear distances were fitted to a bicubic spline which was then interpolated to obtain values needed in the Simpson's rule quadrature of Eq. (5). As a check on this procedure the interpolated values of $I_{lm\mu}$ for 18 eV at the equilibrium geometry of $R_{N\text{-}N} = 2.1273$ a.u. and $R_{N\text{-}O} = 2.2418$ a.u. were found to be within 5% of the values explicitly calculated at this geometry.

III. FIXED-NUCLEI RESULTS

Figure 1 shows our calculated photoionization cross sections for the 7σ level of N_2O at 16 internuclear geometries. The most significant feature of these cross sections is the behavior of the pronounced shape resonance with internuclear goemetry. This resonance moves to lower or higher energies with an increase or decrease respectively in *either* the N–N or N–O bond distance. As can be seen from the appropriate frames of Fig. 1, the position of the resonance depends primarily on the overall length of the molecule and not on the individual N–N and N–O bond distances. It is interesting, however, to compare the position of the σ shape resonance in the 7σ photoionization of N_2O with the σ shape

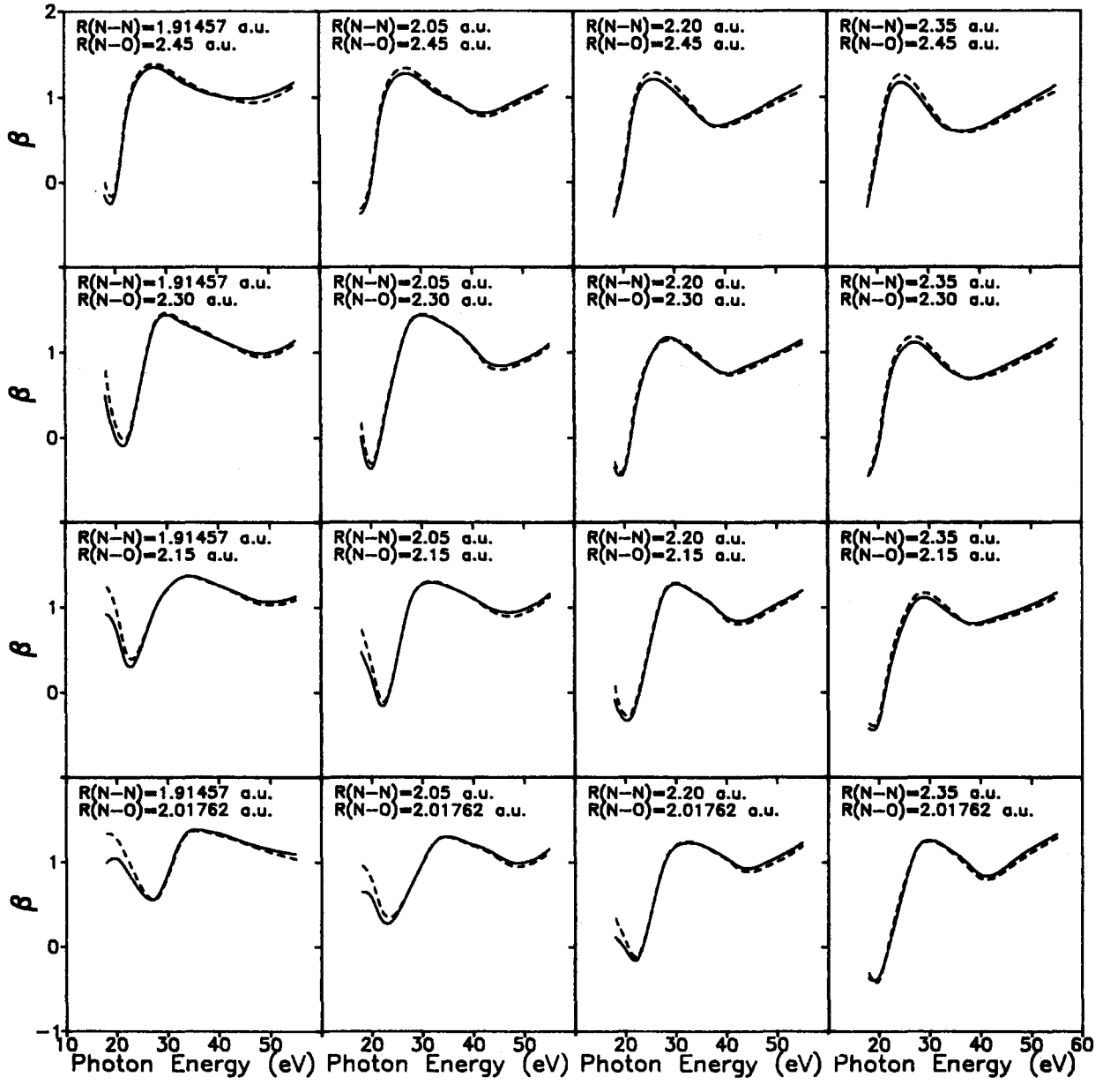

FIG. 3. Photoelectron asymmetry parameters at several internuclear configurations for the $7\sigma^{-1}$ photoionization of N_2O: —, present results (dipole length), ---, present results (dipole velocity). Each frame corresponds to the geometry described in Fig. 1.

resonance in the photoionization cross section of the 5σ level of NO seen at a photoelectron energy of about 7–8 eV.[16,17] The simple model of the shifts in resonance positions with internuclear separation in diatomics[2] would suggest that this σ shape resonance in NO with an R_e of 2.173 a.u. would move down to a photoelectron energy of 3–4 eV for the N–O separation of 2.2418 a.u. in N_2O.[16] Although this relationship is suggestive, the results of Fig. 1 show that this σ shape resonance in N_2O does not behave as though it is localized in the NO bond. In fact, a plot of these resonance positions versus total bond length of the molecule l shows that the photoelectron energy on resonance varies as $1/l^2$, consistent with the naive model of the behavior expected in such a resonance. Finally, the slight enhancement in the cross sections around 35 eV at some internuclear geometries is not shape resonant but arises from the usual energy dependence of the $7\sigma \rightarrow k\pi$ contribution. This feature becomes much less evident as the width of the resonance increases.

Figure 2 shows the eigenphase sum for the $k\sigma$ continuum of the $N_2O(7\sigma^{-1})$ ion at the same internuclear geometries as in Fig. 1. Their behavior shows that there are two shape resonances in this continuum. The low-energy resonance associated with the rise in the eigenphase sum around 20 eV at the equilibrium geometry is seen prominently in the cross sections of Fig. 1. However, the higher shape resonance around 40 eV in the eigenphase sum is completely obscured in the fixed-nuclei cross sections of Fig. 1. We will see shortly that the effect of this resonance is also not evident

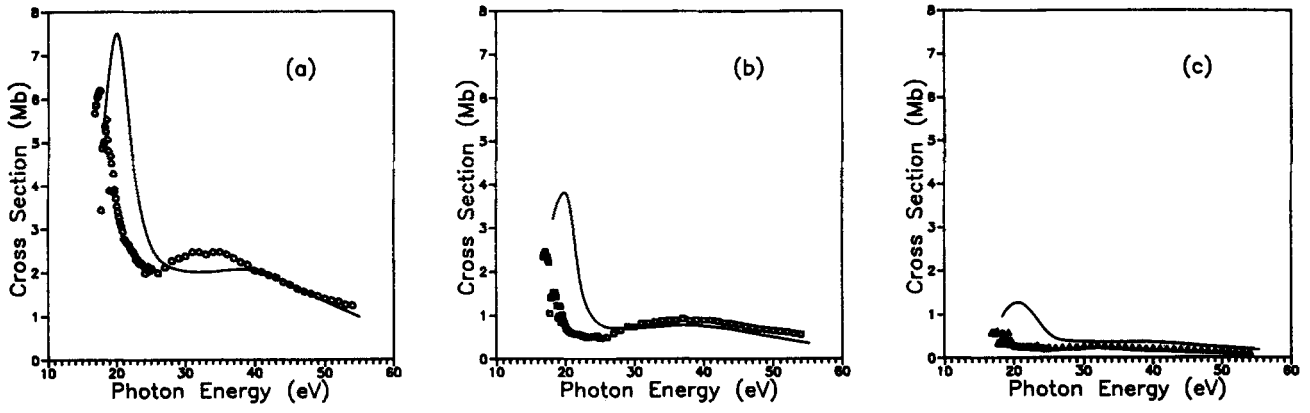

FIG. 4. Cross sections for $7\sigma^{-1}$ photoionization of N_2O to the (000), (100), and (001) vibrational levels of N_2O^+: (a) (000) level; –, present results (dipole length); O, experimental data of Ref. 8; (b) (100) level; –, present results (dipole length); □, experimental data of Ref. 8; (c) (001) level; –, present results (dipole length); △, experimental data of Ref. 8. See the text for explanation of how the experimental data has been normalized.

in the vibrationally resolved cross sections but leads to a broad dip in the photoelectron asymmetry parameters. The behavior of these eigenphase sums with N–N and N–O distances also shows that these resonances cannot be viewed as predominantly associated with either of these two regions of the molecule.

In Fig. 3 we show the fixed-nuclei photoelectron asymmetry parameters for 7σ photoionization at 16 internuclear geometries. The pronounced minimum in these asymmetry parameters at low photoelectron energies is clearly associated with the shape resonance seen in both the cross sections and eigenphase sums of Figs 1 and 2, respectively. These asymmetry parameters also show a broad minimum at higher energy which can be identified as arising from the shape resonance seen at the same energy in the eigenphase sums of Fig. 2. This broad shape resonance produces essentially no enhancement in the fixed-nuclei cross sections.

IV. VIBRATIONALLY RESOLVED RESULTS

Figures 4(a)–4(c) show calculated vibrationally resolved cross sections for photoionization leading to the (000), (100), and (001) levels of the $A\,^2\Sigma^+(7\sigma^{-1})$ state of N_2O^+, respectively. Also shown are the results of Kelly *et al.*[8] derived from ionic fluorescence data (this issue) and normalized to our calculated (000) cross section at 40 eV. Although the physically significant features of these calculated cross sections agree reasonably well with measured relative cross sections, the calculated peak resonance positions are consistently about two eVs too high. We attribute this to inadequacies in our vibrational wave functions, particularly for N_2O^+, for which harmonic potentials were assumed since more refined potentials were not available. In fact, our calculated vibrationally unresolved cross sections show a resonance peak very close in energy to the measured peak position.[10] Comparison of the calculated (000), (100), and (001) cross sections, shifted down by 2 eV so as to bring the peak position of the calculated (000) cross section into agreement with the measured values, with the experimental data in Figs. 5(a)–5(c) also suggests that the potentials assumed here are not too reliable. This example serves to underscore a serious difficulty that will arise in the analysis of vibrationally resolved photoelectron spectra of polyatomic molecules.

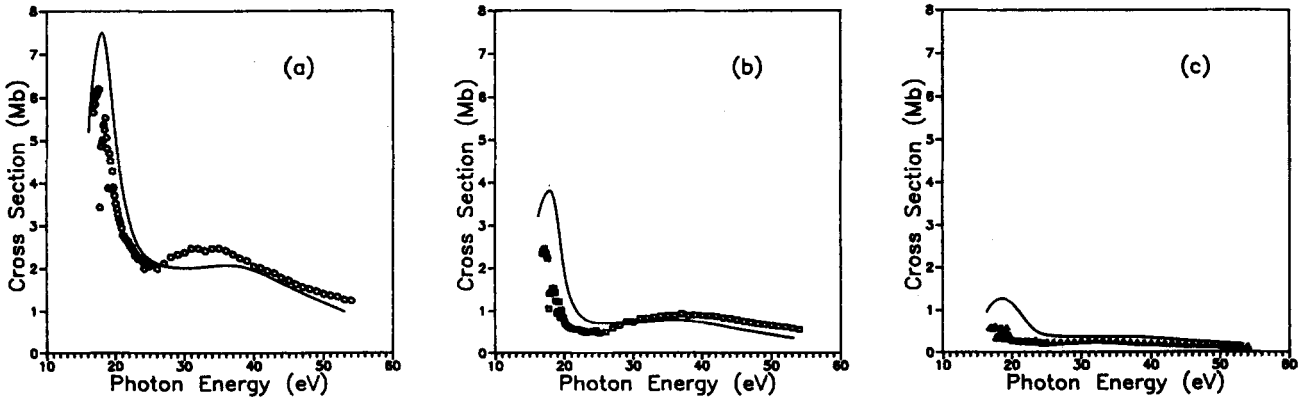

FIG. 5. Comparison of the calculated cross sections for photoionization leading to the (000), (100), and (001) levels of the $A\,^2\Sigma^+(7\sigma^{-1})$ state of N_2O^+, shifted down by 2 eV, with the measured relative values of Ref. 8. See the text for explanation.

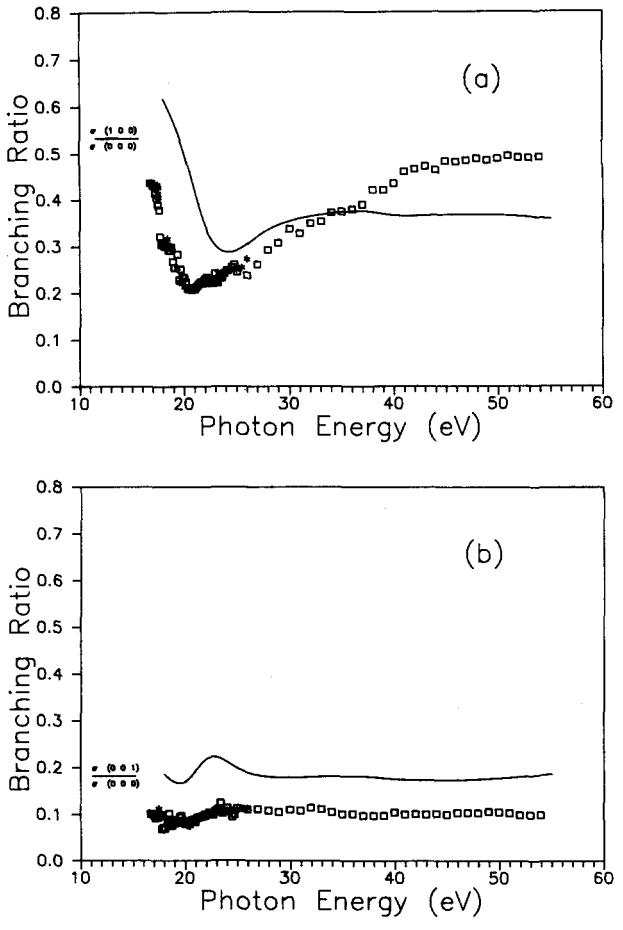

FIG. 6. Vibrational branching ratios (100)/(000) (symmetric stretch) and (001)/(000) (antisymmetric stretch) for $7\sigma^{-1}$ photoionization for N_2O: (a) symmetric stretch; –, present results (dipole length); □, experimental results of Ref. 8; *, experimental results of Ref. 9; (b) antisymmetric stretch; –, present results (dipole length); □, experimental results of Ref. 8; *, experimental results of Ref. 9.

In Figs. 6(a)–6(b) we show our calculated (100)/(000) and (001)/(000) branching ratios for 7σ photoionization of N_2O along with the ionic fluorescence and photoelectron data of Kelly *et al.*[8] and Ferrett *et al.*,[9] respectively. The most significant feature in the (100)/(000) branching ratio is its strong energy dependence (non-Franck–Condon behavior) around a photon energy of about 20 eV which arises from the $k\sigma$ shape resonance seen in the results of Fig. 1. The dip in this calculated branching ratio occurs at higher energy than the one seen experimentally. This discrepancy is probably again due to our use of approximate potentials in obtaining the vibrational wave functions for N_2O^+.[14] In fact, our calculated (100)/(000) branching ratio approaches a Franck–Condon limit significantly different from the experimental value. This discrepancy is another reflection of the limited quality of the available N_2O^+ potential energy curves. The non-Franck–Condon behavior also extends to higher energy—almost to 40 eV—in the measured than in the calculated branching ratios. It is also interesting to speculate whether the behavior seen in the measured branching ratio between 35 and 40 eV arises from the weak σ shape resonance seen at these energies in the eigenphase sums of Fig. 2. Our calculations do show non-Franck–Condon behavior in the branching ratios arising from the $k\sigma$ channel in this energy range, but it is washed out by the large nonresonant $k\pi$ channel.

The (001)/(000) branching ratio also shows non-Franck–Condon behavior around 20 eV which, however, is much less pronounced than in the (100)/(000) branching ratio and also approaches the Franck–Condon value above about 28 eV. The reason for the significantly larger deviations from the Franck–Condon behavior for the symmetric than for the antisymmetric modes can be readily seen from the fixed-nuclei cross sections shown in Fig. 1. These results show that the σ shape resonance moves to lower or higher energies with an increase or decrease respectively in *either* the N–N or N–O bond distance. The resonance hence behaves as though it belongs to the entire molecule and its position and width depend to a great extent on the overall length of the molecule. In the antisymmetric mode, (001), the total bond length of the molecule does not change much and hence the influence of the resonance on its vibrational branching ratio is less pronounced than for the symmetric

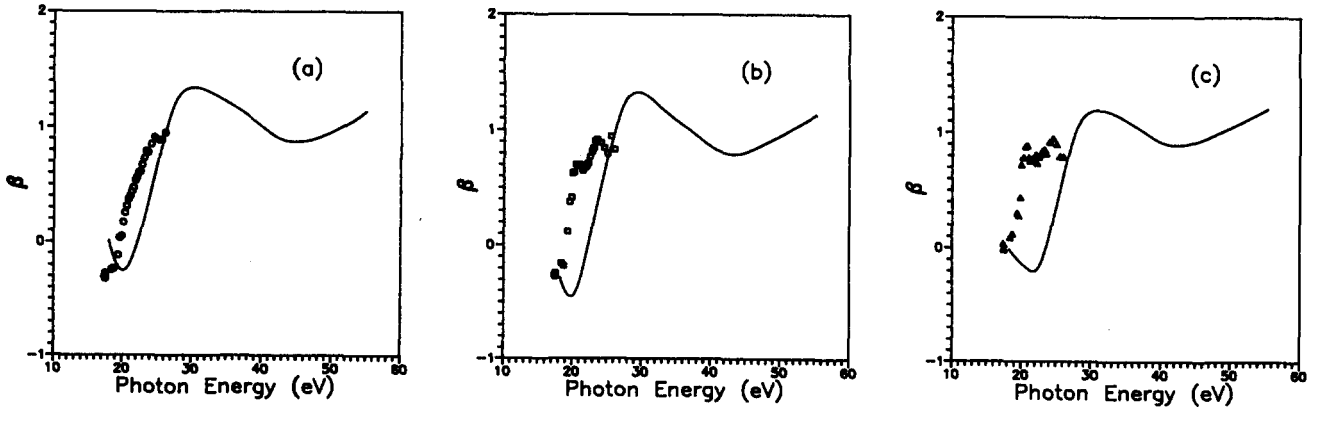

FIG. 7. Photoelectron asymmetry parameters for $7\sigma^{-1}$ photoionization of N_2O: (a) (000) level; —, present results (dipole length); ○, experimental data of Ref. 9; (b) (100) level; —, present results (dipole length); □, experimental data of Ref. 9; (c) (001) level; — present results (dipole length); △, experimental data of Ref. 9.

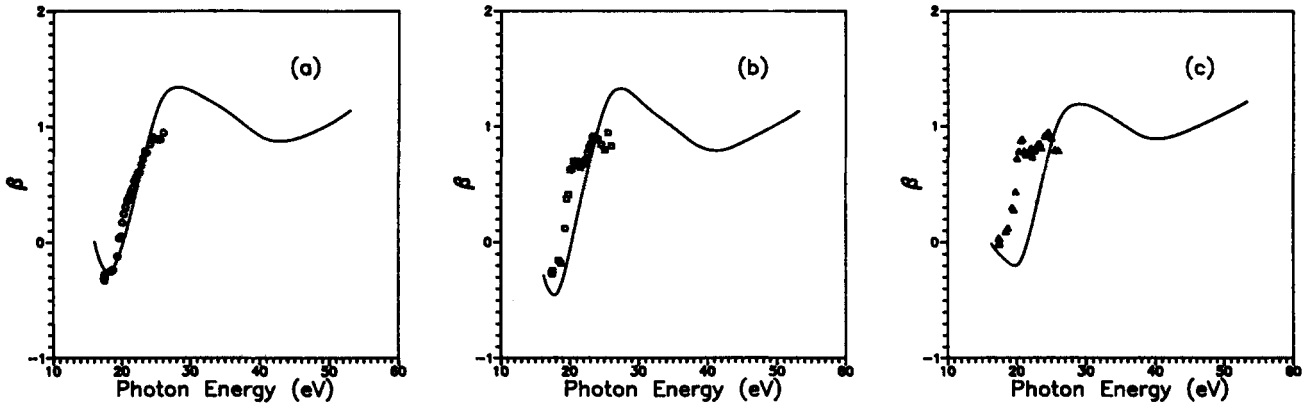

FIG. 8. Comparisons of the calculated asymmetry parameters for photoionization leading to the (000), (100), and (001) levels of the $A\,^2\Sigma^+(7\sigma^{-1})$ state of N_2O^+, shifted down by 2 eV, with the measured values of Ref. 9. See the text for explanation.

stretching mode, (100), where vibrational motion involves changes in the total bond length. These results provide an interesting example of how shape resonances can distinctly influence alternative vibrational modes in polyatomics.

Our calculated photoelectron asymmetry parameters for the (000), (100), and (001) levels are shown in Figs. 7(a)–7(c) along with the measured values of Ferrett *et al.*[9] The calculated asymmetry parameters show clear evidence of the low-energy shape resonance around 20 eV, in general agreement with the experimental data. These calculated asymmetry parameters also show a broad minimum around 40 eV which arises from the higher shape resonance seen in the eigenphase sums and asymmetry parameters of Figs. 2 and 3, respectively. No experimental data is available in this energy range. As in the vibrationally resolved cross sections of Figs. 4(a)–4(c), the strong dip in the asymmetry parameters also occurs at a slightly higher energy than in the experimental data. This difference again is probably due to our use of harmonic potentials in obtaining the vibrational wave functions. Purely for suggestive reasons we compare these vibrationally resolved photoelectron angular distributions, shifted to lower energy by 2 eV [the same as was done for the resonance peaks in Figs. 5(a)–5(c)] with the experimental values in Figs. 8(a)–8(c).

V. CONCLUDING REMARKS

We have studied the vibrationally resolved cross sections and photoelectron asymmetry parameters for photoionization leading to the (000), (100), and (001) levels of the $A\,^2\Sigma^+(7\sigma^{-1})$ state of N_2O^+. One of the main objectives of these studies was to provide some insight into shape resonance behavior for alternative internuclear configurations in polyatomics and hence to predict the expected influence of these resonances on specific vibrational branching ratios. Coupled with the experimental studies reported in the accompanying papers, these results provide an example of the rich dynamical behavior of shape resonances that can be expected in polyatomics. An important conclusion of these studies is that the more pronounced deviations of the vibrational branching ratios observed for the symmetric than for the antisymmetric stretching mode in the region of the low-energy σ shape resonance is essentially due to the fact that this shape resonance behaves as though it belongs to the molecule as a whole and hence its position and width depend on the overall length of the molecule and not on the specific N–N or N–O bond distances. It is clear that vibrationally resolved studies of the photoionization of polyatomic molecules, as illustrated here for N_2O, will provide new insight into molecular photoionization dynamics.

ACKNOWLEDGMENTS

This material is based upon research supported by the National Science Foundation under Grant No. CHE8521391. The authors also acknowledge use of the resources of the San Diego SuperComputer Center which is supported by the National Science Foundation. We would like to thank Dr. E. Poliakoff of Boston University and Dr. T. Ferrett at the National Bureau of Standards for their helpful discussions and for making the results of their experiments available before publication. Finally, we thank Dr. A. D. McLean for providing us with SCF wave functions for N_2O at many geometries.

[1]See, for example, J. L. Dehmer, A. C. Parr, and S. H. Southworth, in *Handbook of Synchrotron Radiation*, edited by G. V. Marr (North-Holland, Amsterdam, 1987), Vol. II.
[2]J. L. Dehmer, D. Dill, and S. Wallace, Phys. Rev. Lett. **43**, 1005 (1979).
[3]J. B. West, A. C. Parr, B. E. Cole, D. L. Ederer, R. Stockbauer, and J. L. Dehmer, J. Phys. B **13**, L105 (1980).
[4]G. Raseev, H. Le Rouzo, and H. Lefebvre-Brion, J. Chem. Phys. **72**, 5701 (1980).
[5]R. R. Lucchese and V. McKoy, J. Phys. B **14**, L629 (1981).
[6]For C_2N_2, as an example, see D. M. P. Holland, A. C. Parr, D. L. Ederer, J. B. West, and J. L. Dehmer, Int. J. Mass. Spectrom. Ion Phys. **52**, 195 (1983); D. L. Lynch and V. McKoy, J. Chem. Phys. **84**, 5504 (1986).
[7]E. D. Poliakoff, M. H. Ho, M. G. White, and G. E. Leroi, Chem. Phys. Lett. **130**, 91 (1986).

[8]L. A. Kelly, L. M. Duffy, B. Space, E. D. Poliakoff, P. Roy, S. H. Southworth, and M. G. White, J. Chem. Phys. **90**, 1544 (1989).
[9]T. A. Ferrett, A. C. Parr, S. H. Southworth, J. E. Hardis, and J. L. Dehmer, J. Chem. Phys. **89**, 1551 (1989).
[10]M. Braunstein and V. McKoy, J. Chem. Phys. **87**, 224 (1987).
[11]M. E. Smith, R. R. Lucchese, and V. McKoy, Phys. Rev. A **29**, 1857 (1984).
[12]A. D. McLean and M. Yoshimine, *Tables of Linear Molecular Wave Functions* (IBM Research Laboratories, San Jose, 1967), pp. 196–204.
[13]A. D. McLean (private communication).
[14]J. H. Callomon and F. Creutzberg, Philos. Trans. R. Soc. London, Ser. A **277** 157 (1974).
[15]E. B. Wilson, Jr., J. C. Decius, and P. C. Cross, *Molecular Vibrations* (Dover, New York, 1955).
[16]T. Gustafsson and H. J. Levinson, Chem. Phys. Lett. **78**, 28 (1981).
[17]M. E. Smith, V. McKoy, and R. R. Lucchese, J. Chem. Phys. **82**, 4147 (1986).